Zou and Xu
Low-carbon Materials and Green Construction (2024) 2:24
https://doi.org/10.1007/s44242-024-00057-3

Low-carbon Materials
and Green Construction

ORIGINAL ARTICLE

Open Access

Mitigating drying shrinkage and efflorescence in high strength alkali-activated materials through steam curing

Shuai Zou[1*] and Bowen Xu[2]

Abstract

The manufacturing of Ordinary Portland Cement (OPC) significantly contributes to global carbon dioxide (CO_2) emissions, necessitating the exploration of alternative binders like alkali-activated materials (AAM). Despite its environmental benefits, AAM generally faces challenges such as drying shrinkage and efflorescence, limiting its industrial application. This study focuses on investigating the impact of steam curing on addressing these challenges in high strength slag-based AAM. The results indicates that high strength AAM can be developed by carefully optimizing the activator-to-binder and water-to-binder ratios, and incorporating steam curing. Specifically, a compressive strength of 112.4 MPa was achieved after one day of steam curing, compared to 100.8 MPa after 28 days of standard curing. This demonstrates the ability of steam curing to accelerate strength development of AAM. Furthermore, steam curing proved to be highly effective in reducing drying shrinkage, which was decreased from 17 351 microstrains to 1 440 microstrains. This reduction aligns the shrinkage levels of AAM with those of OPC, addressing a major limitation of AAM. This study also found that efflorescence was notably mitigated, with a significant reduction observed after a 24-hour steam curing period. These findings highlight steam curing as a cost- effective and practical-effective method in improving the performance of AAM. By addressing the key challenges, steam curing facilitates the broader adoption of AAM in sustainable construction practices.

Keywords Alkali-activated materials, Steam curing, Drying shrinkage, Efflorescence, Low-carbon

摘要

普通硅酸盐水泥的生产是全球二氧化碳排放的重要来源，因此，急需探索碱激发材料等替代胶凝材料。尽管碱激发材料具有显著的环保效益，但其在干燥收缩和泛碱等方面的问题限制了其在工业中的广泛应用。本研究旨在探讨蒸汽养护对高强度矿渣基碱激发材料在上述问题中的影响。研究结果表明，通过调整激发剂/粘合剂及水/粘合剂的比例，并引入蒸汽养护，可以成功研发出高强度的碱激发材料。具体而言，该碱激发材料在经过1天的蒸汽养护后，抗压强度可达112.4 MPa，而标准养护条件下需28天才能达到100.8 MPa。这表明蒸汽养护有助于加速碱激发材料的强度发展。此外，蒸汽养护在减少干燥收缩方面表现出显著效果，将干燥收缩从17351 με降至1440 με。这使碱激发材料的收缩率达到了普通硅酸盐水泥的水平，解决了其一个主要缺陷。研究还发现，经过24小时的蒸汽养护后，泛碱现象明显减轻。这些发现表明，蒸汽养护是一种经济，实用且有效的方法，能够显著提升碱激发材料的性能。通过解决干燥收缩和泛碱等关键问题，蒸汽养护有助于推动碱激发材料在可持续建筑领域的更广泛应用。

关键词 碱激发材料，蒸养，干缩，泛碱，低碳

*Correspondence:
Shuai Zou
frank-s.zou@connect.polyu.hk
Full list of author information is available at the end of the article

1 Introduction

The production of Ordinary Portland Cement (OPC) has been reported to contribute around 8% of the total global carbon dioxide (CO_2) emission [1, 2]. Under the sustainable development background of carbon peak and carbon neutral, alternative lower CO_2 emission binders and aggregates are therefore needed to meet the demand for the construction industry [3, 4]. Alkali-activated materials (AAM), largely made of recycling materials [5] and formed by the reaction between alkali activator and aluminosilicate precursors, has been reported to emerge as a novel and low-CO_2 binder which shows the capacity to replace conventional OPC [6]. Accordingly, AAM has the capacity of reducing the CO_2 emission of OPC production by 80% [7]. Except for the eco-friendly feature, AAM also possesses advantages in early mechanical properties [8], high temperature resistance [9], acid attack resistance [10–12], etc.

Nevertheless, the drawbacks, such as large drying shrinkage [13] and excessive efflorescence [14], of AAM restrict their broader industry applications [15]. Accordingly, the drying shrinkage of AAM is three to ten times than that of OPC [16]. This is commonly explained by the reason that the water is not directly involved in chemical reactions to produce aluminosilicate gel in the AAM system [17]. As a result, the high-increased capillary stress caused by the evaporation of water in the pores eventually leads to the relatively larger drying shrinkage and cracking of AAM [18]. Meanwhile, the efflorescence of AAM refers to the phenomenon that occurs when free alkalis move through the pore to the surface and react with CO_2 in the environment under certain humidity. Excessive efflorescence in AAM can reduce its durability by deteriorating the mechanical properties because of crystallization and microstructural changes [14, 19]. Thus, the research on the mitigation of drying shrinkage and efflorescence of AAM plays an important role in its practical applications.

In fact, several strategies have been utilized to control and mitigate the drying shrinkage and efflorescence of AAM. For instance, Fu et al. [20] investigated the effect of different contents and molecular weights of polypropylene glycol, as a shrinkage reducing admixture, on the drying shrinkage of slag-based AAM. The results indicated that polypropylene glycol showed a high shrinkage mitigation efficiency in the AAM system with mechanism attributed to the combinational effects of surface tension reduction of pore solution and coarsening of pore structure. Besides, Qu et al. tried to mitigate both the autogenous shrinkage and the drying shrinkage of AAM by biofilm [21]. Results showed that adding biofilm increased the hydrophobicity of the pore wall, which in turn decreased the capillary tension. The hydrophobic modification by the biofilm significantly reduced the water loss from AAM to its direct environment (up to 86% at 35 days exposure). Consequently, both autogenous shrinkage and drying shrinkage of AAM were dramatically reduced.

Except for the researches of shrinkage control, Najafi et al. [22] incorporated Al-rich mineral admixtures, such as metakaolin, ground granulated blast-furnace slag, and three types of calcium aluminate cements, into the dry binder to control the efflorescence of AAM based on natural pozzolan. Results showed that calcium aluminate cements exhibited the greatest effect in the efflorescence mitigation by releasing high amounts of alumina into the aluminosilicate AAM gel. Meanwhile, positive effect of hydrothermal curing at elevated temperatures on the efflorescence mitigation of AAM was also indicated in this study. Also, detailed research was conducted by Longhi et al. [23, 24] from the perspective of mechanism and mitigating approaches of efflorescence in metakaolin-based AAM with different alkali concentrations in the alkali activator and substitution (blast furnace slag, silica fume, calcium aluminate cement, silicone oil and a dispersive admixture). The results confirmed that the efflorescence of AAM may be mitigated by controlling the amount of soluble silicates and reducing free alkali cations.

From the above literature review, it can be found that several methods have been applied to alleviate the mentioned two challenges of AAM and positive effects have been achieved. However, from the perspective of practical and broader industry application, safety, economy and convenience are the primary considerations [25]. Compared with the mentioned methods, steam curing is proposed and preferred in this study to solve the both challenges of drying shrinkage and efflorescence for AAM because of its low cost and easy operation. Actually, according to statistics, large parts of the precast concrete components adopt steam curing method in practical production to alleviate the drawbacks of the conventional cast-in-place ready-mixed concrete construction, such as environmental pollution, by-products, intensive labor, and low efficiency [26]. The prefabricated construction technology, which uses components made off-site in a factory and then transported put together on-site to create a structure, is commonly regarded as an effective way for practical construction [27]. Thus, precast AAM treated with steam curing might also provide an easy-operation and effective solution for the practical applications of AAM by overcoming the mentioned challenges.

Actually, some studies have delved into the impact of steam curing on the drying shrinkage and efflorescence of AAM. On the one hand, Aydın and Baradan [28] conducted a study to investigate the mechanical and microstructural properties of heat cured alkali-activated slag mortars, which proved that steam curing was significantly effective in terms of reducing drying shrinkage of alkali-activated slag mortars. The research of Wu et al. [29] also indicated that steam curing can reduce the shrinkage rate of AAM from 64.8% to 68.4% when comparing to ambient curing. Furthermore, a literature review did by Athira et al. [30] confirmed this result, too. On the other hand, Mierzwiński and Walter [31] explored the effect of hydrothermal curing on the efflorescence formation in AAM and demonstrated that steam curing led to a decrease in efflorescence occurrences due to the enhanced binding of alkali ions within the material matrix. The steam curing process was observed to promote the formation of stable hydration products, thereby reducing the availability of free alkalis for efflorescence. Collectively, these studies emphasized the beneficial effects of steam curing on mitigating drying shrinkage and efflorescence in AAM and underscored the importance of considering steam curing as a promising strategy to enhance the practical implementation of AAM in the construction industry. However, the research on investigating the combined impact of steam curing on both drying shrinkage and efflorescence in AAM especially with high compressive strength is still limited.

The aim of this study is to investigate the combined effect of steam curing on the drying shrinkage and efflorescence of high strength AAM. In order to develop high strength AAM, the effect of activator compositions with different ratios of activator/binder and water/binder as well as different curing conditions on the compressive strength development were firstly researched. And then, the drying shrinkage and efflorescence of the high strength AAM with/without steam curing were comparatively investigated with high strength cement mortar. The results showed that steam curing could make the drying shrinkage and efflorescence of high strength AAM to be comparable with that of OPC mortar. This method is low-cost and easy to be operated, which is believed to provide a choice for the application of AAM as binder materials.

2 Experimental programs

2.1 Materials and curing methods

In this study, ground granulated blast furnace slag (GGBS) sourced from Guangdong Shaoguan Iron & Steel Co., Ltd of Mainland China, metakaolin (MK) from TRUTH HOLD of Mainland China, and silica fume (SF) of ELKEM MICROSILICA® 920 were used as the aluminosilicate precursors of AAM. Their chemical compositions were characterized by X-ray fluorescence using a Rigaku Supermini200 spectrometer and the results were listed in Table 1. Detailed comparisons of particle size distribution is presented in Fig. 1. The sodium silicate solution (water glass) was used as the activator which is a commercially sourced and composed of 28.3% SiO_2, 8.6% Na_2O and 58.4% H_2O. Additional sodium hydroxide analytical reagent was added into the sodium silicate solution to adjust its molar modular into 1.4.

Based on the mentioned raw materials, the mix proportions of the prepared GGBS-MK-SF blended AAM mortar was shown in Table 2. For the preparation of testing samples, the dry powder materials were pre-mixed for 3 min in a laboratory mixer. After that, the sodium silicate solution and water were firstly mixed together and then added into the mixer for 2 min low-speed mixing and 3 min high-speed mixing. Finally, the well-mixed mixtures were cast into steel molds, followed by a compacting process of vibrating for 30 s. Plastic sheets were used to cover the surface of the samples to avoid moisture loss. After 24 h, the samples were demolded and then transferred to the environments of temperature 20 ± 2 °C and humidity 95% ± 5% for standard curing as well as 80 ℃ chamber for steam curing, respectively.

2.2 Testing methods

2.2.1 Compressive strength

According to the standard of BS EN 12390–3 [32], the prepared cube specimens with the dimension of 40 × 40 × 40 mm^3 were utilized for the compressive test. During the testing process, the loading rate was set as 0.6 MPa/s.

2.2.2 Drying shrinkage

According to the standard of BS EN 12390–16 [33], 3 prismatic specimens with the dimension of 25 × 25 × 285 mm^3 and an effective gage length of 250 mm were cast

Table 1 Chemical composition of GGBS, MK, and SF (Mass content, %)

Material	SiO2	Al2O3	CaO	MgO	SO3	Fe2O3	K2O	TiO2	LOI
GGBS	30.5	13.4	42.3	8.36	3.09	0.26	0.44	1.33	1.32
MK	52.8	42.0	0.43	-	-	2.50	0.28	2.04	0.94
SF	95.8	0.27	1.10	0.59	0.36	0.13	1.18	/	0.57

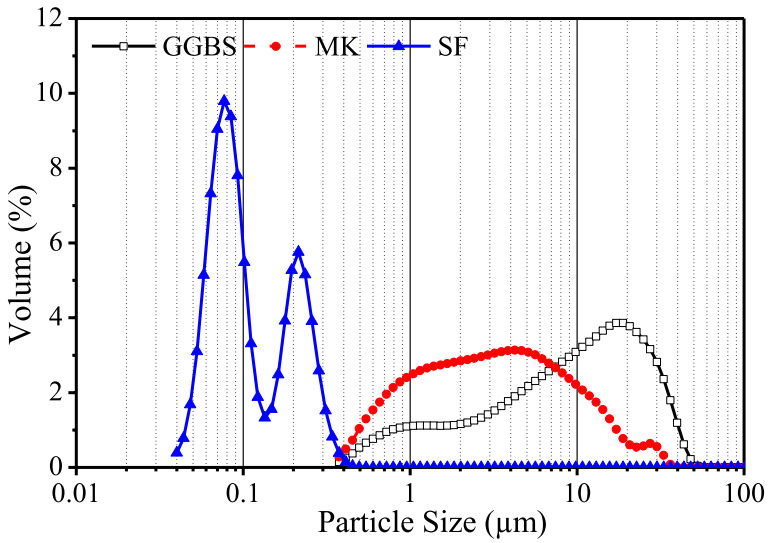

Fig. 1 Particle size distribution of GGBS, MK, and SF

Table 2 Mix design of AAM mortar (g)

Mix	GGBS	MK	SF	Fine aggregate	Water glass	Water	Activator/Binder	Water/Binder	Curing condition
M1	850	100	50	1500	340	110	0.15	0.30	Steam
M2	850	100	50	1500	455	45	0.20	0.30	Steam
M3	850	100	50	1500	568	0	0.25	0.30	Steam
M4	850	100	50	1500	340	160	0.15	0.35	Steam
M5	850	100	50	1500	455	95	0.20	0.35	Steam
M6	850	100	50	1500	568	32	0.25	0.35	Steam
M7	850	100	50	1500	340	210	0.15	0.40	Steam
M8	850	100	50	1500	455	145	0.20	0.40	Steam
M9	850	100	50	1500	568	82	0.25	0.40	Steam
M10	850	100	50	1500	568	0	0.25	0.30	Standard
M11	850	100	50	0	568	0	0.25	0.30	Standard

for the drying shrinkage test. After being casted for 24 h, the specimens were demolded to measure the initial length. And then, the specimens were treated with/without steam curing and stored in the standard curing box (with temperature of 20 ± 2 °C and humidity of 50% ± 5%) for the subsequent measurement.

2.2.3 Efflorescence

To assess the efflorescence of the GGBS-MK-SF AAM, cylindrical specimens with a diameter of 28 mm and a height of 55 mm were prepared with/without steam curing. After that, these specimens were respectively put at concrete standard curing condition of temperature 20 ± 2 ℃ and humidity 95%, as well as room condition with water to immerse the specimens for 4–5 mm depth for efflorescence observation with a period of 28 days. To maintain the water immersing level of the specimens, additional water was daily added to make up with the water absorption and evaporation.

3 Results

3.1 High strength AAM

3.1.1 Effect of activator/binder and water/binder ratios

The diagram depicted in Fig. 2 illustrates the impact of varying activator-to-binder and water-to-binder ratios on the compressive strength of the GGBS-MK-SF blended AAM subjected to a 28-day standard curing period. Examination of the graph reveals a significant influence exerted by the water-to-binder ratio on the compressive strength of the AAM, indicating a notable decline as the water-to-binder ratio increases. This phenomenon can be elucidated by the fact that an elevated water-to-binder ratio within the AAM results in heightened porosity, a compromised interfacial zone,

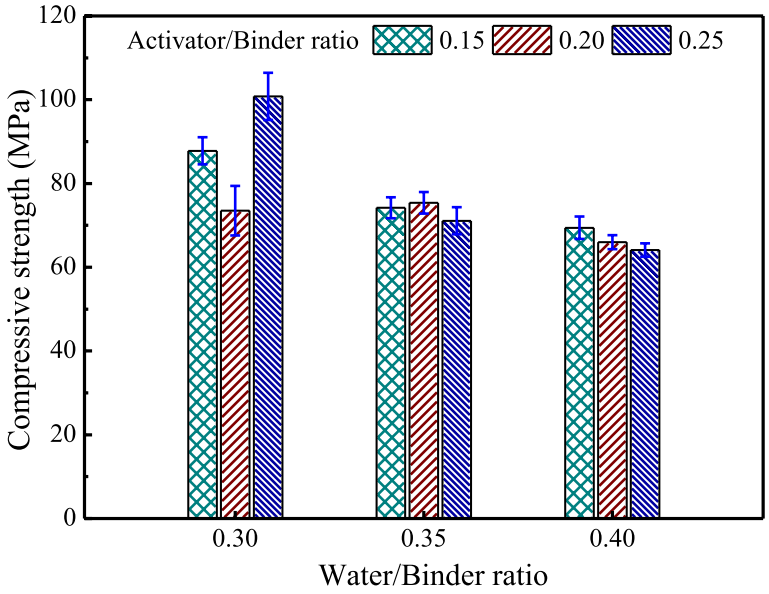

Fig. 2 Effect of activator/binder and water/binder ratios on the compressive strength

and the formation of capillary pores, collectively contributing to a reduction in compressive strength [34, 35]. Specifically, the average compressive strengths of the GGBS-MK-SF blended AAM were recorded at 87.4 MPa, 73.6 MPa, and 66.5 MPa for water-to-binder ratios of 0.30, 0.35, and 0.40, respectively. Notably, the peak compressive strength of 100.8 MPa was achieved at a water-to-binder ratio of 0.30 in conjunction with an activator-to-binder ratio of 0.25.

The activator-to-binder ratio also yielded a considerable impact on the compressive strength of the AAM, with its influence varying across different water-to-binder ratios as shown in Fig. 2. The most pronounced effects of the activator-to-binder ratio were observed in AAM specimens featuring a water-to-binder ratio of 0.30, displaying the lowest value of 73.5 MPa at an activator-to-binder ratio of 0.20 and the highest value of 100.8 MPa at an activator-to-binder ratio of 0.25. However, the optimal compressive strengths of AAM specimens with water-to-binder ratios of 0.35 and 0.40 were achieved at activator-to-binder ratios of 0.20 and 0.15, respectively. This underscores that an excessive activator content may detrimentally impact the compressive strength of the AAM. Consequently, the findings underscore the potential for formulating high-strength AAM through meticulous mix design, underscoring the critical importance of judiciously regulating both water-to-binder and activator-to-binder ratios in AAM formulations to uphold optimal strength characteristics throughout construction processes [36].

3.1.2 Effect of curing conditions

The graphic representation in Fig. 3 delineates the impact of various curing methodologies and durations on the compressive strength of the GGBS-MK-SF AAM. The findings underscore the substantial influence of the chosen curing method on the AAM's compressive strength, with steam curing emerging as a method capable of significantly expediting strength development. Specifically, the AAM subjected to a 3-h steam curing process in this investigation achieved a compressive strength of 78.1 MPa, surpassing the 62.3 MPa strength of the 7-day standard-cured sample, although falling short of the 100.8 MPa strength exhibited by the

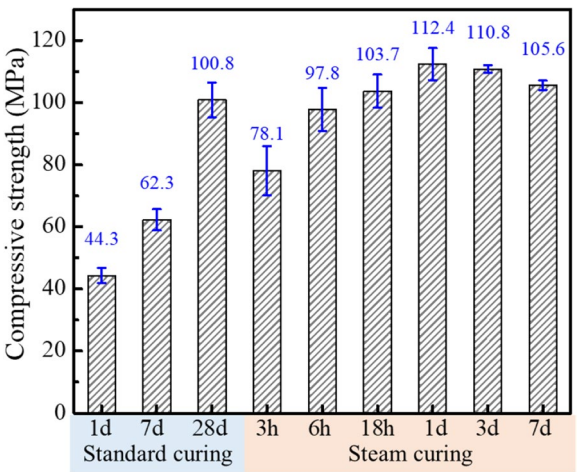

Fig. 3 Effect of curing conditions on the compressive strength

28-day standard-cured sample. Extending the steam curing period to 6 h resulted in the AAM reaching a compressive strength of 97.8 MPa, nearly aligning with the strength of the 28-day standard-cured sample.

Additionally, as the steam curing duration was prolonged to 18 h, the compressive strength of the steam-cured AAM exceeded that of the 28-day standard-cured sample, culminating in the highest compressive strength observed in this study at 112.4 MPa following 1 day of steam curing. These outcomes demonstrate the substantial capacity of steam curing to accelerate the development of AAM strength, thereby facilitating reduced curing times and enhancing construction efficiency [37]. However, it is crucial to note that excessive steam curing can lead to a detrimental impact on AAM strength. As evidenced in this study, AAM specimens subjected to steam curing for 3 and 7 days displayed diminished compressive strength compared to those cured for 1 day.

In conclusion, steam curing proves to be a highly effective method for bolstering AAM strength development; nevertheless, careful regulation of the curing duration is imperative to achieve optimal strength properties.

3.2 Drying shrinkage

3.2.1 Serious drying shrinkage behavior

As demonstrated and substantiated in Fig. 4 (which is the middle part of dying shrinkage testing specimens with length of 285 mm), AAM commonly exhibit substantial drying shrinkage under standard curing conditions. The presence of visible cracks on the specimen's surface, along with noticeable specimen distortion due to shrinkage, highlights significant challenges inherent in AAM compositions. These conspicuous indicators of shrinkage-induced cracking not only impact the aesthetic quality of the material but also impose noteworthy limitations on the practical application of AAM.

Previous research [38] indicates that this shrinkage is predominantly influenced by the evaporation of excess water during the curing process, resulting in volume reduction as the material dries. Furthermore, chemical reactions within the AAM structure can lead to molecular rearrangements, fostering a denser matrix and subsequent shrinkage. The absence of internal reinforcement further exacerbates the susceptibility of AAM to drying shrinkage. To address drying shrinkage in AAM, several methods can be employed: adjusting formulation parameters such as activator-to-binder ratios and water content to minimize shrinkage tendencies [39], incorporating fibers or additives to enhance tensile strength and reduce shrinkage [40, 41], ensuring appropriate temperature, humidity, and curing duration [42], and integrating internal reinforcements or aggregates to counteract shrinkage forces and enhance overall durability [43].

3.2.2 Effect of aggregate and steam curing

Figure 5 illustrates the impact of aggregate presence and steam curing on mitigating drying shrinkage in AAM. The data indicates a substantial drying shrinkage in the AAM paste, reaching 17 351 microstrains after 28 days of curing—a value nearly 30 times higher than that typically observed in conventional normal concrete. This significant shrinkage aligns with the pronounced crack formation and shrinkage behavior depicted in Fig. 4. An analysis of the drying shrinkage progression reveals that the initial 3 days represent the period of most rapid shrinkage development. Specifically, the 3-day drying shrinkage of the AAM paste subjected to standard curing conditions amounted to 14 182 microstrains,

Fig. 4 Serious drying shrinkage behavior of AAM under standard curing

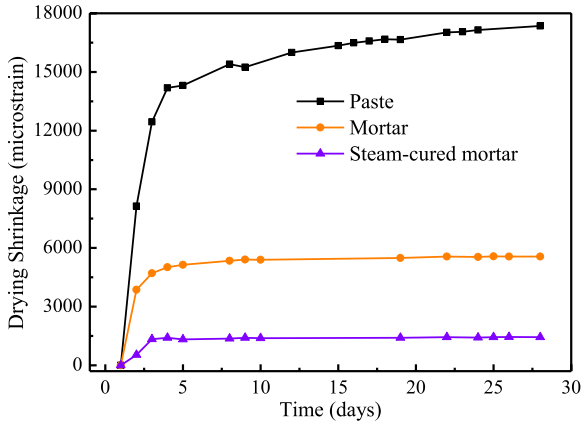

Fig. 5 Effect of aggregate and steam curing on the drying shrinkage of AAM

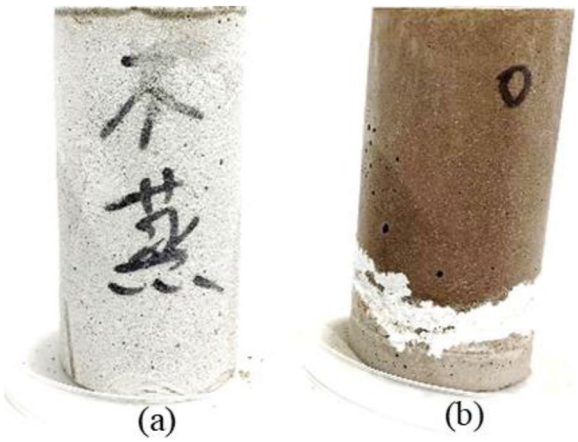

Fig. 6 Efflorescence phenomenon of AAM. **a** standard curing with 95% humidity. **b** water half-immersing environment

constituting approximately 81.7% of the total drying shrinkage observed at the end of the 28-day curing period. This underscores the critical importance of effective shrinkage control during the early stages of AAM development and curing processes.

Furthermore, comparative analysis reveals that the incorporation of aggregate and implementation of steam curing in AAM formulations effectively reduce drying shrinkage. In the context of standard curing conditions for AAM paste, both strategies result in a notable decline in drying shrinkage levels. Specifically, at the 3-day mark, the drying shrinkage decreases from 14 182 microstrains to 5 014 microstrains with the addition of aggregate, and to 1 407 microstrains with the application of steam curing. Similarly, the 28-day drying shrinkage diminishes from 17 351 microstrains to 5 558 microstrains and 1 440 microstrains, respectively, with the same interventions. These findings underscore the efficacy of aggregate inclusion and steam curing in mitigating the substantial drying shrinkage typically observed in AAM, thereby bringing the overall shrinkage levels to a more manageable and acceptable range.

3.3 Efflorescence

3.3.1 Efflorescence phenomenon

In addition to the significant drying shrinkage observed in AAM under standard curing conditions, another intriguing phenomenon that can occur is efflorescence, as shown in Fig. 6. Efflorescence is a crystalline deposit that appears on the surface of materials like AAM, akin to a white, powdery residue. This phenomenon is often associated with the migration of soluble salts to the surface through capillary action as water evaporates, leaving behind these salt deposits upon drying [44]. Just as drying shrinkage can lead to visible cracks and distortion in AAM specimens, efflorescence can mar the surface appearance and compromise the material's aesthetic appeal. Both phenomena underscore the inherent challenges faced in the practical application of AAM compositions. Research indicates that efflorescence in AAM can be influenced by various factors, including the composition of the AAM mix, curing conditions, and environmental exposure [45]. Addressing efflorescence requires a comprehensive understanding of these factors and the implementation of appropriate mitigation strategies to maintain the visual integrity and long-term performance of AAM products in diverse engineering and construction settings.

3.3.2 Effect of steam curing

Steam curing was employed in this research to mitigate the occurrence of efflorescence in AAM specimens, yielding demonstrably positive outcomes, as depicted in Fig. 7. Analysis of the results showcased a stark disparity between AAM samples subjected to standard curing conditions and those treated with steam curing. Specifically, the AAM paste lacking steam curing exhibited pronounced efflorescence when exposed to both water half-immersion and standard curing environments characterized by 95% humidity levels. However, following a brief steam curing period of 24 h, a notable reduction in efflorescence was observed in AAM samples under water half-immersion conditions, with a significant mitigation of efflorescence evident in specimens exposed to the 95% humidity environment. These findings underscore the efficacy of steam curing in alleviating efflorescence formation, primarily attributed to its role in expediting and regulating the curing process, thereby engendering a denser and less permeable AAM matrix. The diminished likelihood of efflorescence emergence can be also attributed to

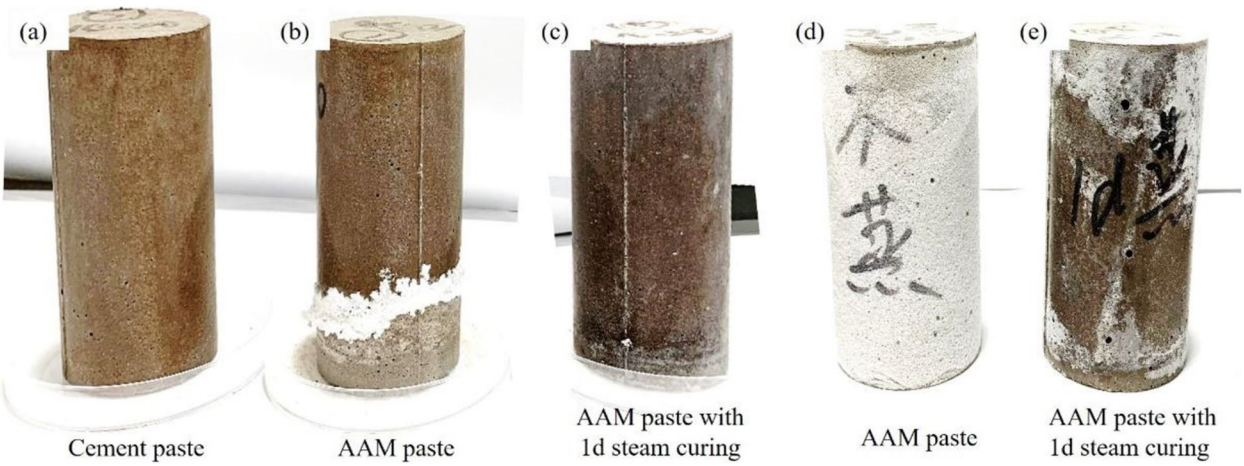

Fig. 7 Effect of steam curing on the efflorescence of AAM under water half-immersing environment (**a** Cement paste. **b** AAM paste. and **c** AAM paste with 1 d steam curing.), and standard curing with 95% humidity environment (**d** AAM paste. **e** AAM paste with 1 d steam curing)

the restricted migration of soluble salts to the surface of the AAM [46]. Consequently, steam curing emerges as a pragmatic and efficacious technique for managing drying shrinkage and efflorescence in AAM applications, offering a straightforward and effective method for enhancing the durability and performance of AAM structures.

4 Discussion

Growing body of literature highlights the environmental and performance advantages of AAM over traditional OPC, particularly in the context of reducing carbon dioxide emissions. However, the practical application of AAM has been hindered by issues such as drying shrinkage and efflorescence, which this study sought to mitigate through steam curing.

4.1 Drying shrinkage mitigation

The results demonstrate that steam curing significantly reduces the drying shrinkage of AAM, bringing it to levels comparable with OPC mortar. This is particularly noteworthy given the substantial shrinkage typically observed in AAM, as evidenced by the 17 351 microstrains recorded under standard curing conditions. The incorporation of aggregates and the application of steam curing were both effective in reducing shrinkage, with steam curing proving to be the more effective of the two. Steam curing reduces drying shrinkage in slag-based AAM can be attributed to the following reasons: (i) accelerated chemical reactions during hydration promote a compact, homogeneous structure, decreasing overall shrinkage; (ii) faster, uniform curing minimizes internal stresses, lowering the risk of cracking and shrinkage during drying; (iii) enhanced early-age strength development makes the material more resistant to deformation and cracking, further reducing drying shrinkage.

4.2 Efflorescence reduction

Efflorescence, another significant challenge in AAM applications, was also effectively mitigated through steam curing. The study revealed that steam curing not only reduces the visible efflorescence on the surface of AAM specimens but also enhances the overall aesthetic and structural integrity of the material. Steam curing reduces efflorescence in slag AAM through a few key mechanisms. Firstly, it speeds up hydration, creating a denser microstructure that hinders salt migration. Secondly, it promotes a less porous material, limiting water and salt movement. Additionally, the controlled curing environment minimizes salt migration to the surface. Lastly, by sealing the surface effectively, steam curing reduces moisture ingress, a common trigger for efflorescence. The findings suggest that steam curing can serve as a practical solution for managing efflorescence, thereby enhancing the durability and visual appeal of AAM products.

4.3 Implications for industry application

The implications of these findings are significant for the broader adoption of AAM in the construction industry. The ability to effectively manage drying shrinkage and efflorescence through steam curing addresses two of the primary barriers to the widespread use of AAM. Moreover, steam curing is a cost-effective and easily implementable method, aligning with industry needs for practical and economical solutions. Given that large parts of precast concrete components already utilize steam curing, the transition to steam-cured AAM components could be seamless, promoting sustainable construction practices.

4.4 Future research directions

While this study provides compelling evidence for the benefits of steam curing, further research is needed to optimize the curing parameters and explore the long-term performance of steam-cured AAM in various environmental conditions. Additionally, investigating the interplay between different AAM formulations and steam curing could yield insights into tailoring the process for specific applications. Understanding the microstructural changes induced by steam curing at a molecular level could also enhance the development of more robust and durable AAM.

5 Conclusion

This study provides compelling evidence for the effectiveness of steam curing in overcoming the significant challenges of drying shrinkage and efflorescence in high strength alkali-activated materials (AAM). The following conclusions can be draw from this study:

(i) By carefully optimizing the activator-to-binder and water-to-binder ratios, and incorporating steam curing into the process, the compressive strength of AAM was markedly enhanced. Remarkably, the compressive strength reached an impressive 112.4 MPa after just one day of steam curing, highlighting the rapid strength development facilitated by this method.

(ii) Steam curing proved to be highly effective in reducing drying shrinkage. The shrinkage was dramatically decreased from an initial 17 351 microstrains to just 1 440 microstrains, bringing it in line with the levels typically observed in cement mortar. This reduction is particularly noteworthy as it addresses one of the primary limitations of AAM.

(iii) Steam curing effectively mitigated the issue of efflorescence, especially under conditions of high humidity. This mitigation not only improves the aesthetic quality of the AAM surfaces but also shows the potential in enhancing their long-term durability and performance.

These findings underscore the potential of steam curing as a practical and economical solution for enhancing the performance of AAM. Looking ahead, future research should prioritize the optimization of steam curing parameters to further refine this technique. Additionally, exploring the long-term durability and performance of steam-cured AAM under various environmental conditions will be crucial. Such investigations will provide deeper insights and support the broader industrial application of AAM, reinforcing their role as a viable and sustainable option in the construction industry.

Acknowledgements
The authors would like to express their gratitude to the support of The Hong Kong Polytechnic University and Xi'an Jiaotong-Liverpool University.

Authors' contributions
Shuai Zou: Methodology, Data curation, Investigation, Original draft;Bowen Xu: Methodology, Reviewing and Editing.

Funding
The article was funded by 'Micro-structural, thermal and mechanical properties of concrete incorporating recycled materials (PGRS2012023)' and The Hong Kong Polytechnic University.

Data availability
Data and material will be made available on reasonable request.

Declarations

Competing interests
The authors affirm that they have no known financial interests or personal relationships that could have influenced the findings presented in this paper.

Author details
[1]Department of Civil and Environmental Engineering, The Hong Kong Polytechnic University, Hong Kong, China. [2]Department of Civil Engineering, Design School, Xi'an Jiaotong-Liverpool University, Suzhou, China.

Received: 14 November 2024 Revised: 30 November 2024 Accepted: 3 December 2024
Published online: 23 December 2024

References

1. York, I., & Europe, I. (2021). Concrete needs to lose its colossal carbon footprint. *Nature, 597*(7878), 593–594.
2. Huang, L., Krigsvoll, G., Johansen, F., Liu, Y., & Zhang, X. (2018). Carbon emission of global construction sector. *Renewable and Sustainable Energy Reviews, 81*, 1906–1916.
3. Xiao, J. Z., & Zou, S. (2024). Cement at 200: Towards net-zero fully recycled concrete. *Nature, 631*, 740.
4. Zou, S., Sham, M. L., Xiao, J., Leung, L. M., Lu, J.-X., & Poon, C. S. (2024). Biochar-enabled carbon negative aggregate designed by core-shell structure: A novel biochar utilizing method in concrete. *Construction and Building Materials, 449*, 138507.
5. Mohajerani, A., Suter, D., Jeffrey-Bailey, T., Song, T., Arulrajah, A., Horpibulsuk, S., & Law, D. (2019). Recycling waste materials in geopolymer concrete. *Clean Technologies and Environmental Policy, 21*, 493–515.
6. Davidovits, J. (2013). Geopolymer cement, A review. *Geopolymer Institute, Technical papers, 21*, 1–11.
7. Zakka, W. P., Lim, N. H. A. S., & Khun, M. C. (2021). A scientometric review of geopolymer concrete. *Journal of Cleaner Production, 280*, 124353.
8. Neupane, K., Chalmers, D., & Kidd, P. (2018). High-strength geopolymer concrete-properties, advantages and challenges. *Advances in Materials, 7*(2), 15–25.
9. Çelikten, S., Sarıdemir, M., & Özgür Deneme, İ. (2019). Mechanical and microstructural properties of alkali-activated slag and slag + fly ash mortars exposed to high temperature. *Construction and Building Materials, 217*, 50–61.
10. Ren, J., Guo, S.-Y., Su, J., Zhao, T.-J., Chen, J.-Z., & Zhang, S.-L. (2019). A novel TiO2/Epoxy resin composited geopolymer with great durability in wetting-drying and phosphoric acid solution. *Journal of Cleaner Production, 227*, 849–860.
11. Ren, J., Zhang, L., Walkley, B., Black, J. R., & San Nicolas, R. (2022). Degradation resistance of different cementitious materials to phosphoric acid attack at early stage. *Cement and Concrete research, 151*, 106606.
12. Aiken, T. A., Kwasny, J., Sha, W., & Soutsos, M. N. (2018). Effect of slag content and activator dosage on the resistance of fly ash geopolymer binders to sulfuric acid attack. *Cement and Concrete Research, 111*, 23–40.

13. Khan, I., Xu, T., Castel, A., Gilbert, R. I., & Babaee, M. (2019). Risk of early age cracking in geopolymer concrete due to restrained shrinkage. *Construction and Building Materials, 229*, 116840.
14. Zhang, Z., Wang, H., Provis, J. L., & Reid, A. (2013). Efflorescence: A critical challenge for geopolymer applications? *Concrete Institute of Australia's Biennial National Conference 2013*University of Southern Queensland.
15. Kadhim, A., Mankhi, B. S., & Al-Bujasim, M. (2024). Review of Geopolymer Technology, Barriers and Limitations. *Al-Mustaqbal Journal of Sustainability in Engineering Sciences, 2*(1), 4.
16. Mastali, M., Kinnunen, P., Dalvand, A., Firouz, R. M., & Illikainen, M. (2018). Drying shrinkage in alkali-activated binders–a critical review. *Construction and Building Materials, 190*, 533–550.
17. Cui, C., Tai, W., Luo, C., Wang, L., & Peng, H. (2024). Mechanisms underlying drying shrinkage in ASM-based geopolymer: Capillary tensile stress and its prediction method. *Construction and Building Materials, 450*, 138698.
18. Yang, Y., Chen, Z., Feng, W., Nong, Y., Yao, M., & Tang, Y. (2021). Shrinkage compensation design and mechanism of geopolymer pastes. *Construction and Building Materials, 299*, 123916.
19. Wu, B., Li, L., Deng, H., Zheng, Z., Xiang, Y., Li, Y., & Ma, X. (2022). Characteristics and mechanism of efflorescence in fly ash-based geopolymer mortars under quasi-natural condition. *Journal of Building Engineering, 55*, 104708.
20. Fu, C., Ye, H., Lei, A., Yang, G., & Wan, P. (2020). Effect of novel superabsorbent polymer composites on the fresh and hardened properties of alkali-activated slag. *Construction and Building Materials, 232*, 117225.
21. Qu, Z., Yu, Q., Ji, Y., Gauvin, F., & Voets, I. K. (2020). Mitigating shrinkage of alkali activated slag with biofilm. *Cement and Concrete Research, 138*, 106234.
22. Kani, E. N., & Allahverdi, A. (2011). Investigating shrinkage changes of natural pozzolan based geopolymer cement paste. *Iranian Journal of Materials Science and Engineering, 8*(3), 50–60.
23. Longhi, M. A., Zhang, Z., Rodríguez, E. D., Kirchheim, A. P., & Wang, H. (2019). Efflorescence of alkali-activated cements (geopolymers) and the impacts on material structures: A critical analysis. *Frontiers in Materials, 6*, 89.
24. Longhi, M. A., Rodriguez, E. D., Walkley, B., Eckhard, D., Zhang, Z., Provis, J. L., & Kirchheim, A. P. (2022). Metakaolin-based geopolymers: Efflorescence and its effect on microstructure and mechanical properties. *Ceramics International, 48*(2), 2212–2229.
25. Zou, S., Chau, C. K., Leung, L. M., Duan, Z., Xiao, J., Sham, M. L., & Poon, C. S. (2024). Developing low-carbon high-strength core-shell aggregates using solid waste by cold-bonding techniques. *Construction and Building Materials, 416*, 135116.
26. Yee, A. A., & Eng, P. H. D. (2001). Social and environmental benefits of precast concrete technology. *PCI journal, 46*(3), 14–19.
27. Priya, P. K., Neamitha, M. (2018). A review on precast concrete. *International Journal of Engineering and Technology (IRJET), 5*(1).
28. Aydın, S., & Baradan, B. (2012). Mechanical and microstructural properties of heat cured alkali-activated slag mortars. *Materials & Design, 35*, 374–383.
29. Wu, R., Gu, Q., Gao, X., Huang, J., Guo, Y., & Zhang, H. (2024). Effect of curing conditions on the alkali-activated blends: Microstructure, performance and economic assessment. *Journal of Cleaner Production, 445*, 141344.
30. Athira, V. S., Bahurudeen, A., Saljas, M., & Jayachandran, K. (2021). Influence of different curing methods on mechanical and durability properties of alkali activated binders. *Construction and Building Materials, 299*, 123963.
31. Mierzwiński, D., Walter, J. (2019). Autoclaving of alkali-activated materials. *IOP Conference Series: Materials Science and Engineering* (p. 012012). IOP Publishing.
32. B. EN. (2019). 12390–3 Testing hardened concrete. Compressive strength of test specimens.
33. B. EN. (2019). 12390–16 Testing hardened concrete Determination of the shrinkage of concrete.
34. Kurhade, S. D., Patankar, S. V. (2023). Effect of water-to-binder (W/B) ratio and various zones of river sand on properties of geopolymer concrete. *Materials Today: Proceedings*.
35. Yang, K.-H., Cho, A.-R., & Song, J.-K. (2012). Effect of water–binder ratio on the mechanical properties of calcium hydroxide-based alkali-activated slag concrete. *Construction and Building Materials, 29*, 504–511.
36. Nodehi, M., & Aguayo, F. (2021). Ultra high performance and high strength geopolymer concrete. *Journal of Building Pathology and Rehabilitation, 6*(1), 34.
37. Nurruddin, M. F., Sani, H., Mohammed, B. S., & Shaaban, I. (2018). Methods of curing geopolymer concrete: A review. *International Journal of Advanced and Applied Sciences, 5*(1), 31–36.
38. Trincal, V., Multon, S., Benavent, V., Lahalle, H., Balsamo, B., Caron, A., Bucher, R., Caselles, L. D., & Cyr, M. (2022). Shrinkage mitigation of metakaolin-based geopolymer activated by sodium silicate solution. *Cement and Concrete Research, 162*, 106993.
39. Huang, W., & Wang, H. (2024). Formulation development of metakaolin geopolymer with good workability for strength improvement and shrinkage reduction. *Journal of Cleaner Production, 434*, 140431.
40. Zhang, B., Zhu, H., Feng, P., & Zhang, P. (2022). A review on shrinkage-reducing methods and mechanisms of alkali-activated/geopolymer systems: Effects of chemical additives. *Journal of Building Engineering, 49*, 104056.
41. Frayyeh, Q. J., & Kamil, M. H. (2021). The effect of adding fibers on dry shrinkage of geopolymer concrete. *Civil Engineering Journal, 7*(12), 2099–2108.
42. Wallah, S. E. (2009). Drying shrinkage of heat-cured fly ash-based geopolymer concrete. *Modern Applied Science, 3*(12), 14–21.
43. Al-Hedad, A. S., Farhan, N. A., Zhang, M., Sheikh, M. N., & Hadi, M. N. (2020). Effect of geogrid reinforcement on the drying shrinkage and thermal expansion of geopolymer concrete. *Structural Concrete, 21*(3), 1029–1039.
44. Ge, Y., Tian, X., Huang, D., Zhong, Q., Yang, Y., & Peng, H. (2023). Understanding efflorescence behavior and compressive strength evolution of metakaolin-based geopolymer under a pore structure perspective. *Journal of Building Engineering, 66*, 105828.
45. Kani, E. N., Allahverdi, A., & Provis, J. L. (2012). Efflorescence control in geopolymer binders based on natural pozzolan. *Cement and Concrete Composites, 34*(1), 25–33.
46. Zhou, S., Zhou, S., Zhang, J., Tan, X., & Chen, D. (2020). Relationship between moisture transportation, efflorescence and structure degradation in fly ash/slag geopolymer. *Materials, 13*(23), 5550.

Publisher's Note